Sweat Gland Tumors Arising on Acral Sites: A Molecular Survey

Thibault Kervarrec, Anne Tallet, Nicolas Macagno, Arnaud de la Fouchardière, Daniel Pissaloux, Franck Tirode, Ignacio Bravo, Alain Nicolas, Sylvain Baulande, Pierre Sohier, et al.

Sweat gland tumors arising on acral sites: a molecular survey.

Thibault Kervarrec[1-3], Anne Tallet[4], Nicolas Macagno[1,5,6], Arnaud de la Fouchardière[1,7,8], Daniel Pissaloux[7,8], Franck Tirode[8], Ignacio G. Bravo[9], Alain Nicolas[11], Sylvain Baulande[11], Pierre Sohier[1,12,13], Brigitte Balme[1,16], Amélie Osio[1,14], Marie-Laure Jullie[29], Isabelle Moulonguet[15], Benjamin Bonsang[1,19], Emilie Tournier[1,20], Michael Herfs[22], Eric Frouin[23], Anoud Zidan[24], Eduardo Calonje[24], Patricia Berthon[3], Antoine Touzé[3], Alice Seris[1,26], Laurent Mortier[1,27], Thomas Jouary[1,26], Bernard Cribier[1,28], Maxime Battistella[1,14].

1: CARADERM, French network of rare cutaneous cancer, France.
2: Department of Pathology, University hospital center of Tours, Tours, France
3: "Biologie des infections polyomavirus" team, UMR INRA ISP1282, University of Tours, France
4: Platform of Solid Tumor Molecular Genetics, University hospital center of Tours, Tours, France
5: Department of Pathology, APHM, Timone University Hospital, Marseille, France
6: Aix Marseille Univ, INSERM, MMG, UMR1251, Marmara Institute, Marseille, France
7: Department of Biopathology, Center Léon Bérard, Lyon, France
8: University of Lyon, Université Claude Bernard Lyon 1, INSERM 1052, CNRS 5286, Centre Léon Bérard, Cancer Research Center of Lyon, Equipe Labellisée Ligue contre le Cancer, Lyon, France
9: French National Center for Scientific Research (CNRS), Laboratory MIVEGEC (CNRS IRD Univ Montpellier), Montpellier, France.
10: Infections and Cancer Biology Group, International Agency for Research on Cancer, Lyon, France
11: Institut Curie, PSL Research University, CNRS UMR3244, 75248, Paris, France
12: Faculté de Médecine Paris Centre Santé, University of Paris, Paris, France
13: Department of Pathology, Cochin Hospital, AP-HP, AP-HP.Centre-Université de Paris, Paris, France
14: Department of Pathology, Hopital Saint Louis, AP-HP Universite´ Paris 7, Paris,
15: Cabinet Mathurin Moreau, Paris, France
16: Department of Pathology, University hospital center of Lyon-Sud, Hospices Civils de Lyon, Lyon, France.
17: Department of Pathology, University hospital center of Bordeaux, Pessac, France.
18: Cypath Lyon, Villeurbanne, France.
19: Department of Pathology, Hôpital Ambroise Pare, AP-HP, Paris, France
20: Department of Pathology, CHU Toulouse, Institut Universitaire du Cancer de Toulouse Oncopole, Toulouse, France_ Université Toulouse III Paul Sabatier, Toulouse, France.
21: Department of Pathology, University hospital center of Clermont-Ferrand, Clermont-Ferrand, France.
22: Laboratory of Experimental Pathology, GIGA-Cancer, University of Liège, Liège, Belgium
23: Department of Pathology, University hospital center of Poitiers, LITEC, UR 15560, University of Poitiers, Poitiers, france
24: Dermatopathology Laboratory, St John's Institute of Dermatology, St Thomas' Hospital, London, UK
25: Department of Dermatology, University hospital center of Tours, Tours, France
26: Department of Dermatology, Hospital center of Pau, Pau, France
27: Department of Dermatology, University hospital center of Lille, Lille, France
28: Clinique dermatologique, Hôpitaux Universitaires & Université de Strasbourg, Hôpital Civil, Strasbourg, France
29: Dermatopathology Laboratory, St John's Institute of Dermatology, St Thomas' Hospital, London, UK

Disclosure/Conflict of Interest: The authors declare no conflict of interest.
Sources of support: CARADERM Network

Institutional review board: The local Ethics Committee in Human Research of Tours (France) approved the study (no. ID RCB2009-A01056-51)
Patient consent statement: a no-objection form was sent to all participants.

Corresponding author:
Dr. Thibault Kervarrec
Department of Pathology, Hôpital Trousseau, CHRU de Tours, 37044 TOURS France. Tel: +33 (2) 47 47 80 69/Fax: +33 (2) 47 47 46 22
Email: thibaultkervarrec@yahoo.fr

Running Title: Acral sweat gland tumors: a molecular survey

Manuscript Word count (Excluding capsule summary, abstract, references, figures, and tables)**: 2500. Abstract: 243.**
List of attachments: Figures: 5, Tables: 2, Supplements (supplementary methods: 4, supplementary tables: 5, supplementary figures: 4)

Abstract

Background: recurrent oncogenic drivers have been identified in several sweat gland tumors. In particular, integration of human papillomavirus type 42 (HPV42) has recently been reported in digital papillary adenocarcinoma (DPA).

Objectives: the main objectives of the present study were i) to provide an overview of the prevalence of previously identified oncogenic drivers in acral sweat gland tumors and ii) to genetically characterize tumors with not yet identified recurrent genetic alteration.

Methods: cases of acral sweat gland tumors were extracted from the database of the French network CARADERM. After histological review, the presence of previously identified genetic alterations was investigated in the entire cohort (n=79) using a combination of immunohistochemistry, targeted DNA and RNA sequencing. Tumor entities with no recurrent genetic alterations were then submitted to whole-transcriptome sequencing.

Results: *CRTC1::MAML2* fusion was detected in hidradenoma and hidradenocarcinoma (n=9/12 and n=9/12). The p.V600E mutation of *BRAF* was observed in all cases of tubular adenoma (n=4). *YAP1:MAML2* and *YAP1::NUTM1* fusions were observed in poroid tumors (n=15/25). *ETV6::NTRK3* and *TRPS1::PLAG1* fusion transcripts were identified in secretory carcinoma (n=1/1) and cutaneous mixed tumors (n=3/4), respectively. The HPV42 genome was detected in DPA (n=10/11) and in one adnexal adenocarcinoma not otherwise specified (NOS). Finally, whole transcriptome analysis revealed *BRD3::NUTM1* or *NSD3::NUTM1* fusions in two cases of NUT adnexal carcinoma and *NCOA4::RET and CCDC6::RET* fusion transcripts in two cystadenoma/hidrocystoma-like tumors.

Conclusion: our study confirmed that molecular analysis might contribute to the diagnosis of sweat gland tumors arising in acral sites.

Key words: Digital papillary adenocarcinoma, HPV42, Papillomavirus, NUT, RET

Introduction

Due to their relative rarity and the large number of histotypes, the diagnosis of sweat gland tumors is often challenging. Notably on acral sites [1], the distinction is notoriously difficult between digital papillary adenocarcinoma (DPA), a rare and aggressive adnexal tumor with frequent local recurrences and possible metastatic spread [1–3] and other acral sweat gland tumors[1,4], such as hidradenoma, tubular adenoma, hidrocystoma/cystadenoma, mixed tumors and poroid hidradenoma[1–6].

During the last decade, the identification of highly-specific recurrent genetic alterations has been reported in several sweat gland tumors and can help for diagnosis purposes. In particular, rearrangements of *CRTC1::MAML2* and *CRTC3::MAML2* have been identified in hidradenomas[7,8] and hidradenocarcinomas[7,9]. Furthermore, mutations in the MAP kinase pathway, particularly *BRAF p.*V600E, were found in tubular adenomas[10]. More recently, frequent rearrangements of *YAP1::MAML2* and *YAP1::NUTM1* were observed in poroma, and their malignant counterparts[11,12]. In contrast, for a long time, only limited data was available on the genetics of DPA with activating mutation of *BRAF* exceptionally detected in this setting[13–17]. Recently, Thomas Wiesner[18] reported the integration of human papillomavirus type 42 (HPV42) into the tumor cell genome of a cohort of DPA cases, a result recently confirmed by another group[19,20].

Thus, in the present study we aim i) to give an overview of the prevalence of previously identified oncogenic drivers of acral sweat gland tumors, and ii) to genetically characterize the tumor histotypes with not yet identified recurrent genetic alteration.

Methods

Patients and samples

All cases of acral sweat gland tumors (palms and soles) registered in the database of the French network of rare skin cancers, CARADERM[21] between 2015 and 2020 were considered for inclusion (local ethics committee, Tours, France; ID: RCB2009-A01056-51)[22]. Additionally, one case of DPA and one case of hidrocystoma/cystadenoma-like tumor of the digits were extracted from the consultation cases of EC, AZ and ET. Only cases with sufficient tumor material for representative hematein phloxin saffron (HPS) slide staining and DNA extraction were included in the present analysis. All cases were histopathologically reviewed by 2 pathologists (MB, BC).

Clinical and follow-up data

Age, sex, stage according to the American Joint Committee on Cancer (AJCC) at the time of surgery[23], location of the primary tumor and follow-up of the patient were collected from patient files.

Step-by-step investigation of tumor samples

The management of the samples is summarized in **Figure 1/ Flow chart**. Briefly, we have evaluated in the entire cohort the presence of *CRTC1/3::MAML2* fusion, mutation of *BRAF* and HPV42 genome. The cases in which none of these alterations was detected were subsequently screened by immunohistochemistry for rearrangement of *YAP1* and *NUTM1* [11]. The identified cases were further investigated by targeted RNA sequencing (RNA-seq). Mixed tumors and secretory carcinoma cases were also investigated by targeted RNA sequencing, as fusion transcripts involving the *PLAG1*[24] and *NTRK3*[24] genes have been reported in these entities. All DPA samples with sufficient FFPE material, as well as 13 randomly selected (sealed envelopes) non-DPA samples, were submitted to HPV-capture NGS. Whole-transcriptome RNA-sequencing was performed in tumor groups without identified genetic alterations.

Detection of *CRTC1::MAML2 and CRTC3::MAML2* fusion transcripts

All details on the procedures for the detection of *CRTC1::MAML2* and *CRTC3::MAML2* fusion and *BRAF* mutation are available in **Supplementary Method S1**.

In situ hybridization and immunohistochemistry

Detection of HPV42 RNA was performed using the RNAscope® Probe HPV42, (ACD, Bio-Techne SAS, France), according to the manufacturer's instructions (**Supplementary Method S2**). All details regarding immunohistochemical staining are available in **Supplementary Method S2.**

Targeted RNA sequencing

The rearrangements of *NUTM1, YAP1, PLAG1, and NTRK3* were investigated using next-generation sequencing (NGS). The library was prepared using a custom FusionPlex Comprehensive kit (Archer®Dx) and sequenced on a MiSeq System (Illumina). The data obtained were analyzed using Archer Analysis Suite v6.03.2. AMP (Anchored Multiplex PCR) technology.

Whole RNA sequencing

Whole-transcriptome RNA sequencing was performed as previously described[25] (**Supplementary Method S3**).

HPV42 status determination and search for integration

HPV42 status was determined using real time PCR (qPCR) with primers and probe specific of the L1 genomic region. PCR reactions were run on the LightCycler 480 II (Roche diagnostics, Indianapolis, USA). Primer sequences are available in **Supplementary Method S1.** The demonstration of the presence and integration of HPV42 was achieved using HPV Capture-Next generation sequencing as previously described [26] (**Supplementary Method S4)**.

Statistical analyses

Continuous data are described by medians and ranges, and categorical data by percentage of interpretable cases. Associations were assessed by Mann-Whitney and two-tailed Fisher's exact tests for continuous and categorical data, respectively.

Results

Patients' characteristics and histological findings

Among the 158 cases of acral sweat gland tumor registered in the CARADERM database, 79 were included in the present study (**Figure 1/Flow Chart**). The clinical, histopathological, and molecular characteristics of the cases are presented in **Table 1**, **Figure 2**, **Supplementary Table 1** and **Supplementary Figures 1-4**. After histopathological review, the tumors were classified as: DPA (n=11), hidradenoma and hidradenocarcinoma (n=12 and 12 respectively), porocarcinoma (n=18), poroid hidradenoma (n=3), malignant poroid hidradenoma (n=4), tubular adenoma (n=4), cystadenoma/hidrocystoma-like tumors of the digits (n=4 including 2 atypical cases), mixed tumors (n=4), adnexal adenocarcinoma not otherwise specified (NOS) (n=4), cribriform carcinoma (n=1) and secretory carcinoma (n=1).

Briefly, the cases of DPA had a mixed solid, cystic, and papillary architecture with frequent back-to-back gland formation. The cases of Hidradenoma and hidradenocarcinoma had a mostly solid growth pattern and were composed of clear or eosinophilic cells entrapped in a hyalinized stroma. The tubular adenoma consisted of multiple tubular structures with frequent pseudopapillary projections. The association of epithelial, myoepithelial, and mesenchymal components was observed in all mixed tumors. Hidrocystoma/cystadenoma-like tumors were mainly unilocular structures lined by a double layer of myoepithelial and luminal cells. Among the cases classified as porocarcinoma, two cases harbored unusual architectural and cytological findings, as detailed below. A single case was considered ambiguous without a clear distinction between tubular adenoma and DPA (**Supplementary Figure 1**).

Follow-up data were available in 22 cases (median duration: 34 months, ranges: 5-156) (**Supplementary Table 1**). Only four patients developed metastases and two deaths occurred within the observation time. Among these severe cases, three patients had been diagnosed with DPA and one with adnexal adenocarcinoma NOS.

Recurrent genetic alterations in sweat gland tumors

We then evaluated the presence of these previously reported genetic alterations in our cohort (**Figure 1**/**Table 1**). *CRTC1::MAML2* rearrangements were detected only in hidradenoma and hidradenocarcinoma (n=9/12 and n=9/12, 75% respectively) and the *BRAF* p.V600E mutation was observed in all tubular adenoma (n=4/4). Furthermore, an activating *BRAF* mutation was detected in the morphologically ambiguous case mentioned above (**Supplementary Figure 1**). *ETV6::NTRK3* fusion transcript was detected in the secretory carcinoma case, and *TRPS1::PLAG1* fusion transcripts were identified in three of the four cases of cutaneous mixed tumors (75%).

Combined immunohistochemical (**Supplementary Table 2, Supplementary Figure 2**) and molecular analysis further identified *YAP1::MAML2* fusion transcripts in 5 cases of porocarcinoma, while the *YAP1::NUTM1* fusion was detected in all cases of poroid hidradenoma, of their malignant counterpart and in 3 cases of porocarcinoma.

Recurrent HPV42 genome detection in DPA

To assess the potential association of DPA with HPV integration as recently described, real-time PCR detection of the HPV42 genome was applied to the entire cohort (n=79). This analysis confirmed the presence of the HPV42 genome in 10 of the 11 DPA samples. The clinical, and histopathological characteristics of the cases are presented in **Table 2/Supplementary Figure 3**. Among non-DPA samples, the detection of the HPV42 genome was only possible in an undifferentiated tumor diagnosed as adnexal adenocarcinoma NOS (case #12) (**Supplementary Figure 4**).

To further comfort, the implication of HPV42 in DPA oncogenesis, seven cases of DPA (cases #1-7) and 13 samples of randomly selected non-DPA cases (cases #12-24) were submitted to HPV-capture next-generation sequencing. This analysis identified HPV42 sequences in all

samples tested (**Table 2/Figure 3 A-B**) with a higher number of HPV42 reads in DPA cases (median number of HPV42 reads: 155,288; range: 46,418 to 1,296,665) compared to the other tumors (median number of HPV42 reads: 745, range: 380 to 57,555) ($p<10^{-4}$). Importantly, only HPV genotype 42 sequences were present. Integration sites were identified in 3 DPA cases (Cases # 2, 3 and 7) involving non-coding regions in two cases and in intronic sequence of the *FRYL* gene in one case (**Supplementary Table 3**). Furthermore, DPA associated with the episomal form of the virus (4 cases) were characterized by a higher number of HPV reads (Cases #1, 4-6, reads number: 155288-1296665) than HPV integrated tumors (p=0.03). It should be noted that *in situ* detection of HPV42 transcripts (RNA scope) revealed intense positivity in more than 90% of the cells in all tested cases of DPA (n=5) (**Figure 3C, Table 2**), while no signal was observed in 8 of the non-DPA samples included as controls.

Therefore, the high prevalence of the HPV42 genome in DPA and the almost lack in other sweat gland tumors strongly suggest the detection of HPV42 as a highly relevant tool for the diagnosis of DPA in current practice (Sensitivity=91%, Specificity= 99%).

Identification of *BRD3::NUTM1*, *NSD3::NUTM1 in NUT adnexal carcinoma* and *NCOA4::RET, CCDC6::RET* fusion transcripts in hidrocystoma/cystadenoma-like tumors of the digits

In our cohort, two tumor cases, morphologically classified as 'porocarcinoma' due to an infiltrative growth pattern and duct formation, still showed morphological characteristics distinct from other porocarcinoma cases (**Figure 4/Supplementary Table 4**). These specimens were composed of epithelial strands, cords, and tubules with a reticulated growth pattern entrapped in a hyalinized stroma. Tumor cells were medium-sized with large round nuclei, clear chromatin, and prominent nucleoli. Ducts were present in both cases, whereas keratocysts were observed in one. Importantly, immunohistochemistry detected a discordant positivity for YAP1 and NUT in these cases. Accordingly, RNA sequencing revealed *BRD3::NUTM1* and *NSD3::NUTM1* fusion transcripts in these cases, therefore demonstrating that these tumors are cutaneous NUT adnexal carcinomas, a recently described tumor distinct from porocarcinoma.

Finally, whole transcriptome RNA sequencing was performed in tumor groups without identified genetic alteration. No recurrent fusion or mutation was observed in cases of adenocarcinoma NOS (2 analyzed cases). On the contrary, analysis of the two hidrocystoma/cystadenoma-like tumor cases, for which library generation was possible, revealed a *NCOA4::RET* and a *CCDC6::RET* fusion transcript previously described in salivary intraductal carcinoma [27]. Importantly, these tumors (cases #35 and #79/**Figure 5, Supplementary Table 5**) consisted of cystic lesions that formed glands, pseudopapillary projection, and anastomotic epithelial tufts. One case was classified as atypical due to poor circumscription.

Therefore, our results confirmed the existence of primary cutaneous NUT adnexal carcinomas [28] and suggested that *RET* fusions could constitute an oncogenic driver of hidrocystoma/cystadenoma-like tumors of the digits, and we.

Discussion

The oncogenesis of adnexal tumor entites is frequently related to one specific recurrent oncogenic driver, highlighting the diagnostic value of these molecular alterations integrated in a given clinical and morphological context. In the present study, we confirmed the high prevalence of previously identified genetic alterations in hidradenoma and hidradenocarcinoma, tubular adenoma, poroid, and mixed tumors, as well as in secretory carcinoma. We further comforted the recent description of the role of HPV42 in the oncogenesis of DPA by detecting the HPV42 genome in 10 DPA (91%) and showed that the episomal form of the virus could also have oncogenic properties, as previously reported for HPV16[26,29]. Finally, we identified two NUT adnexal carcinomas with *BRD3::NUTM1* or *NSD3::NUTM1* fusion, an extremely rare tumor, and detected *NCOA4::RET and CCDC6::RET* fusions in two hidrocystoma/cystadenoma tumors of the digits.

Hidradenoma is one of the first adnexal tumors for which a recurrent oncogenic event was identified, i.e. *CRTC1::MAML2* fusion. Although previous series reported this alteration in less than 50% of cases of hidradenoma [7,30], Russell-Goldman et al. recently reported the detection of *MAML2* fusion in up to 90% of cases [31] as confirmed in our study. Similarly, by analogy to their salivary counterpart, rearrangements of the *PLAG1* gene have been identified in cutaneous mixed tumors [32,33], as observed in our study that demonstrated *TRPS1::PLAG1* fusion in 75% of the cases, with no morphological specificities in the non-rearranged case. It should be noted that although no cutaneous myoepithelial tumor lacking an epithelial component, i.e. myoepithelioma, was included in our study, the recent series by Mehta et al. demonstrated immunohistochemical expression of PLAG in this setting, which could reflect gene rearrangement [34].

In 2019, Thomas Wiesner reported at the International Society of Dermatopathology conference that HPV42, a “low-risk” HPV[35], could be integrated into the DPA cell genome [18]. Accordingly, the recurrent detection of HPV42 in almost all DPA tested in our cohort,

the high coverage of the entire viral genome by sequencing, as well as the viral integration in some samples strongly supports the contribution of HPV42 to the oncogenesis of DPA. Interestingly, although prominent glandular and papillary structures were observed in most HPV42 positive tumors, therefore classified as DPA, integration of the HPV42 genome was detected in one more sample that consisted of undifferentiated neoplasia (**Supplementary Figure 4**). Therefore, detection of HPV42 in this sample rise the hypothesis of a poorly differentiated DPA.

Among mimickers of DPA, tubular adenoma is genetically characterized by *BRAF* p.V600E mutation [10], while this mutation seems to be rare in DPA (detected in only two cases in the literature) [14,17]. Consequently, this canonical p.V600E mutation of *BRAF* was detected in all cases of tubular adenoma in our study and in one case for which the morphological distinction between DPA and tubular adenoma was considered doubtful (**Supplementary Figure 1**). However, detection of a *BRAF* p.V600E mutation, lack of HPV42 genome and goof outcome (45 months of follow-up without local recurrence) argued in favor of tubular adenoma.

Hidrocystoma/cystadenoma is a benign cystic tumor showing differentiation toward the sweat gland coil. Interestingly, Molina-Ruiz *et al.* reported 7 cases of “Apocrine hidrocystoma and cystadenoma”-like tumors arising in the digits, and proposed that these tumors constituted a variant of DPA [5]. In our study, four cases, including two atypical cases, presented close characteristics to the tumors described by Molina-Ruiz *et al*. Moreover, whole-exome RNA-seq demonstrated *NCOA4::RET* and *CCDC6::RET* fusion transcripts (**Figure 5**) in two of these cases (case #35 and #79), a gene fusion alteration previously reported in intraductal carcinoma of the salivary gland [27]. Therefore, it is likely that some “Apocrine hidrocystoma and cystadenoma”-like tumors represent the cutaneous counterpart of salivary intraductal carcinomas.

Importantly, our study further demonstrated the existence of primary cutaneous NUT carcinoma by identifying *BRD3::NUTM1* and *NSD3::NUTM1* fusion in two adnexal tumors with poroid characteristics (**Figure 4**). Although these cases were initially diagnosed as porocarcinoma based on the association of malignant characteristics and duct formation, these tumors showed microscopic features distinct from porocarcinoma and similar to the one observed in extracutaneous NUT carcinoma [36,37] : prominent nucleoli, clear chromatin, a distinct growth pattern and a combination of ducts and foci of keratinization. Until now, only three potential primary cutaneous NUT carcinomas have been reported [28,38,39]. Identification of additional cases is required to determine which phenotypic characteristics are specific to this entity.

In conclusion, our study confirmed the recurrent presence of HPV42 in DPA, further demonstrated the existence of primary cutaneous NUT adnexal carcinoma and finally evidenced recurrent RET fusion in hidrocystoma/cystadenoma-like tumors of the digits.

Acknowledgments:

The authors thank Anne-Flore ALBERTINI, Khalid ALHAZMI, Frédéric ARCHAMBAUD FERRANTI, Jean-Jacques AUGER, Régine BATTIN-BERTHO, Cindy BERNARD DECOT, Marie-Hélène BIZOLLON, CALES Valérie, Amélie CARBONNELLE-PUSCIAN, Catherine CHAPELIN, Maryline DAUPHIN, Philippe DEBIAIS, Manuela DELAGE-CORRE, Lauriane DEPAEPE, Maryline DOREL, Luc DURAND, Helena FLAMME, William GODARD, Angélique GUILLAUDEAU, Gabrielle Goldman-Levy, Véronique HURIET, Frédérique JOSSIC, Anne-Marie LAGRANGE-CARRE, François LE MARC'HADOUR, Francois LE PELLETIER DE GLATIGNY, Annie LEVY, Ioannis LIOLIOS, Philippe MOGUELET, Damien MOLL, Olivier NOHRA, Romain PERALLON, Laure PINQUIER, Patricia REAU, Pomone RICHARD, Delphine ROCAS, Véronique ROLLAND, Pierre ROMERO, Jacqueline RIVET, Amandine

ROUSSEAU, Wissam SANDID, Frédéric STAROZ, Nora SZLAVIK, Cyprien TILMANT, Priscilla VERHULST Franck VITTE for their help and assistance. High-throughput sequencing was performed by the ICGex NGS platform of the Institut Curie supported by the grants ANR-10-EQPX-03 (Equipex) and ANR-10-INBS-09-08 (France Génomique Consortium) from the Agence Nationale de la Recherche ("Investissements d'Avenir" program), by the ITMO-Cancer Aviesan (Plan Cancer III) and by the SiRIC-Curie program (SiRIC Grant INCa-DGOS- 465 and INCa-DGOS-Inserm_12554).

Disclosure/Conflict of Interest: The authors declare no conflict of interest.

Ethics Approval: The local Ethics Committee in Human Research of Tours (France) approved the study (no. ID RCB2009-A01056-51)

Author Contributions:

TK, AT, BC, MB performed study concept and design; TK, AT, MB performed development of methodology and writing, review and revision of the paper; NM, AF, DP, FT, MT, CC, IB, TG, AN, SB, SL, PS, AC, BC, BB, MLJ, AO, IM, SLR, CC, BB, LL, FF MH, AZ, EC, MS, PG, AT, AS, EF, LM, TJ provided acquisition, analysis and interpretation of data, and statistical analysis; AF, DP, FT, MT, CC, PG, AS provided technical and material support. All authors read and approved the final paper.

Funding: CARADERM Network

Data Availability Statement: The datasets used and/or analyzed during the current study are available from the corresponding author on reasonable request.

Supplements.

Supplementary Method S1. Detection of *CRTC1::MAML2 and CRTC3::MAML2* fusion transcripts and *BRAF* mutation

Supplementary Method S2. RNA scope and immunohistochemistry

Supplementary Method S3. Whole transcriptome RNA sequencing

Supplementary Method S4. HPV42 integration detection

Supplementary Table 1. Clinical features of the cohort

Supplementary Table 2. Expression of YAP1-C ter and NUT in acral tumors

Supplementary Table 3. Characteristics of the HPV42 genomes detected in the cohort

Supplementary Table 4. Characteristics of the two NUT carcinoma included in this study

Supplementary Table 5. Characteristics of the two *RET*-rearranged cystadenoma/hidrocystoma-like tumors of the digits included in this study

Supplementary Figure 1. Morphological features of case #33. Microscopic examination revealed an unusual and difficult to interpret morphology, that included focal pseudopapillary structures and necrosis, complicating the distinction between DPA and tubular adenoma.

Supplementary Figure 2. Morphological and immunohistochemical features of poroid tumor cases. A poroid hidradenoma with NUT expression and a porocarcinoma with loss of YAP1 -C-terminal expression are depicted.

Supplementary Figure 3. Morphological characteristics of case #8 diagnosed as Digital papillary adenocarcinoma but lacking HPV42 genome detection.

Supplementary Figure 4. Morphological characteristics of a HPV42-positive case morphologically diagnosed as adnexal adenocarcinoma not otherwise specified (case #12).

References

1 Kazakov D. Digital papillary adenocarcinoma. In WHO Classification of the Skin Tumors. IARC. WHO. 2018.

2 Kao GF, Helwig EB, Graham JH. Aggressive digital papillary adenoma and adenocarcinoma. A clinicopathological study of 57 patients, with histochemical, immunopathological, and ultrastructural observations. *J. Cutan. Pathol.* 1987; **14**; 129-146.

3 Rismiller K, Knackstedt TJ. Aggressive Digital Papillary Adenocarcinoma: Population-Based Analysis of Incidence, Demographics, Treatment, and Outcomes. *Dermatol Surg* 2018; **44**; 911-917.

4 Wiedemeyer K, Gill P, Schneider M, et al. Clinicopathologic Characterization of Hidradenoma on Acral Sites: A Diagnostic Pitfall With Digital Papillary Adenocarcinoma. *Am J Surg Pathol* 2020; **44**; 711-717.

5 Molina-Ruiz A-M, Llamas-Velasco M, Rütten A, et al. 'Apocrine Hidrocystoma and Cystadenoma'-like Tumor of the Digits or Toes: A Potential Diagnostic Pitfall of Digital Papillary Adenocarcinoma. *Am. J. Surg. Pathol.* 2016; **40**; 410-418.

6 Asgari M, Chen S. Commentary on a Recent Article Entitled 'a Case Report of Papillary Digital Adenocarcinoma With BRAFV600E Mutation and Quantified Mutational Burden'. *Am J Dermatopathol* October 2020.

7 Kazakov DV, Ivan D, Kutzner H, et al. Cutaneous hidradenocarcinoma: a clinicopathological, immunohistochemical, and molecular biologic study of 14 cases, including Her2/neu gene expression/amplification, TP53 gene mutation analysis, and t(11;19) translocation. *Am J Dermatopathol* 2009; **31**; 236-247.

8 Winnes M, Mölne L, Suurküla M, et al. Frequent fusion of the CRTC1 and MAML2 genes in clear cell variants of cutaneous hidradenomas. *Genes Chromosomes Cancer* 2007; **46**; 559-563.

9 Yoshimi K, Goto H, Otsuka M, et al. Translocation of the MAML2 gene in hidradenocarcinoma. *J. Dermatol.* 2017; **44**; e190-e191.

10 Liau J-Y, Tsai J-H, Huang W-C, et al. BRAF and KRAS mutations in tubular apocrine adenoma and papillary eccrine adenoma of the skin. *Hum. Pathol.* 2018; **73**; 59-65.

11 Sekine S, Kiyono T, Ryo E, et al. Recurrent YAP1-MAML2 and YAP1-NUTM1 fusions in poroma and porocarcinoma. *J. Clin. Invest.* 2019; **129**; 3827-3832.

12 Macagno N, Kervarrec T, Sohier P, et al. NUT Is a Specific Immunohistochemical Marker for the Diagnosis of YAP1-NUTM1-rearranged Cutaneous Poroid Neoplasms. *Am J Surg Pathol* February 2021.

13 Surowy HM, Giesen AK, Otte J, et al. Gene expression profiling in aggressive digital papillary adenocarcinoma sheds light on the architecture of a rare sweat gland carcinoma. *Br. J. Dermatol.* 2019; **180**; 1150-1160.

14 Bell D, Aung P, Prieto VG, et al. Next-generation sequencing reveals rare genomic alterations in aggressive digital papillary adenocarcinoma. *Ann Diagn Pathol* 2015; **19**; 381-384.

15 Le LP, Dias-Santagata D, Pawlak AC, et al. Apocrine-eccrine carcinomas: molecular and immunohistochemical analyses. *PLoS One* 2012; **7**; e47290.

16 Dias-Santagata D, Lam Q, Bergethon K, et al. A potential role for targeted therapy in a subset of metastasizing adnexal carcinomas. *Mod Pathol* 2011; **24**; 974-982.

17 Trager MH, Jurkiewicz M, Khan S, et al. A Case Report of Papillary Digital Adenocarcinoma With BRAFV600E Mutation and Quantified Mutational Burden. *Am J Dermatopathol* 2021; **43**; 57-59.

18 Thomas Wiesner. The molecular revolution in Dermatopathology, ISDP, Lisbon. June 2019.

19 Vanderbilt CM, Bowman AS, Middha S, et al. Defining Novel DNA Virus-Tumor Associations and Genomic Correlates Using Prospective Clinical Tumor/Normal Matched Sequencing Data. *J Mol Diagn* March 2022; S1525-1578(22)00067-8.
20 Vanderbilt C, Brenn T, Moy AP, et al. Association of HPV42 with digital papillary adenocarcinoma and the use of in situ hybridization for its distinction from acral hidradenoma and diagnosis at non-acral sites. *Mod Pathol* May 2022.
21 Seris A, Battistella M, Beylot-Barry M, et al. [Creation, implementation and objectives of CARADERM, a national network for rare skin carcinomas - Adnexal neoplasm part]. *Ann Dermatol Venereol* 2019; **146**; 704-710.
22 Gardair C, Samimi M, Touzé A, et al. Somatostatin Receptors 2A and 5 Are Expressed in Merkel Cell Carcinoma with No Association with Disease Severity. *Neuroendocrinology* 2015; **101**; 223-235.
23 Harms KL, Healy MA, Nghiem P, et al. Analysis of Prognostic Factors from 9387 Merkel Cell Carcinoma Cases Forms the Basis for the New 8th Edition AJCC Staging System. *Ann. Surg. Oncol.* 2016; **23**; 3564-3571.
24 Bishop JA, Taube JM, Su A, et al. Secretory Carcinoma of the Skin Harboring ETV6 Gene Fusions: A Cutaneous Analogue to Secretory Carcinomas of the Breast and Salivary Glands. *Am J Surg Pathol* 2017; **41**; 62-66.
25 Macagno Nicolas, Pissaloux Daniel, de la Fouchardière Arnaud. Wholistic approach – transcriptomic analysis and beyond using archival material for molecular diagnosis. *Genes Chromosomes Cancer 2021; (accepted, in Press)*.
26 Holmes A, Lameiras S, Jeannot E, et al. Mechanistic signatures of HPV insertions in cervical carcinomas. *NPJ Genom Med* 2016; **1**; 16004.
27 Skálová A, Ptáková N, Santana T, et al. NCOA4-RET and TRIM27-RET Are Characteristic Gene Fusions in Salivary Intraductal Carcinoma, Including Invasive and Metastatic Tumors: Is 'Intraductal' Correct? *Am J Surg Pathol* 2019; **43**; 1303-1313.
28 Rubio Gonzalez B, Ortiz MV, Ross DS, et al. Skin adnexal carcinoma with BRD3-NUTM2B fusion. *J Cutan Pathol* July 2021.
29 Péré H, Vernet R, Pernot S, et al. Episomal HPV16 responsible for aggressive and deadly metastatic anal squamous cell carcinoma evidenced in peripheral blood. *Sci Rep* 2021; **11**; 4633.
30 Kyrpychova L, Kacerovska D, Vanecek T, et al. Cutaneous hidradenoma: a study of 21 neoplasms revealing neither correlation between the cellular composition and CRTC1-MAML2 fusions nor presence of CRTC3-MAML2 fusions. *Ann Diagn Pathol* 2016; **23**; 8-13.
31 Russell-Goldman E, Hanna J. MAML2 Gene Rearrangement Occurs in Nearly All Hidradenomas: A Reappraisal in a Series of 20 Cases. *Am J Dermatopathol* July 2022.
32 Bahrami A, Dalton JD, Krane JF, et al. A subset of cutaneous and soft tissue mixed tumors are genetically linked to their salivary gland counterpart. *Genes Chromosomes Cancer* 2012; **51**; 140-148.
33 Panagopoulos I, Gorunova L, Andersen K, et al. NDRG1-PLAG1 and TRPS1-PLAG1 Fusion Genes in Chondroid Syringoma. *Cancer Genomics Proteomics* 2020; **17**; 237-248.
34 Mehta A, Davey J, Gharpuray-Pandit D, et al. Cutaneous Myoepithelial Neoplasms on Acral Sites Show Distinctive and Reproducible Histopathologic and Immunohistochemical Features. *Am J Surg Pathol* March 2022.
35 Okodo M, Okayama K, Teruya K, et al. Koilocytic changes are not elicited by human papillomavirus genotypes with higher oncogenic potential. *J Med Virol* March 2020.
36 French CA, Miyoshi I, Kubonishi I, et al. BRD4-NUT fusion oncogene: a novel mechanism in aggressive carcinoma. *Cancer Res.* 2003; **63**; 304-307.
37 Stelow EB, French CA. Carcinomas of the upper aerodigestive tract with

rearrangement of the nuclear protein of the testis (NUT) gene (NUT midline carcinomas). *Adv Anat Pathol* 2009; **16**; 92-96.
38 Kervarrec Thibault, Amatore Florent, Lehmann-che Jacqueline, et al. Expanding the morphological spectrum of primary cutaneous NUT carcinoma with BRD3-NUTM1 fusion. *American Journal of Surgical Pathology*.
39 Nishimura Y, Ryo E, Yamazaki N, et al. Cutaneous primary NUT carcinoma with BRD3-NUTM1 fusion. *American Journal of Surgical Pathology*.

Legends

Table 1. Genetic characteristics of the cohort according to tumor types.

Table 2. Clinical, microscopic, immunohistochemical and molecular characteristics of DPA.

Figure 1. Flow chart.

*Additional targeted RNA sequencing analyzes were further performed in mixed tumors and secretory carcinoma for which rearrangements of *PLAG1, EWSR and NTRK3* genes have been reported.

Figure 2. Representative illustrations of digital papillary adenocarcinoma (DPA) and confounders. A DPA, a hidradenocarcinoma a tubular adenoma, a poroid adenoma a secretory carcinoma and a mixed tumor are depicted. DPA harbors combined solid, cystic and papillary growth patterns with frequent back-to back glands. Hidradenocarcinoma consists in a poorly delimitated proliferation of clear cells entrapped in a hyalinized stroma. Tubular adenoma consists in a proliferation of non-atypical, cuboid cells forming tubes and pseudopapillary projections. Poroid hidradenoma is a deep located nodular neoplasm composed of poroid and cuticular cells. Fused tubular structures contaning eosinophilic secretion products are observed in secretory carcinoma. Mixed tumor is characterized by the presence of epithelial, myoepithelal and mesenchymal component.

Figure 3. Identification of HPV42 in digital papillary adenocarcinoma (DPA) and non-DPA samples by capture-NGS and *in situ* hybridization. A. Identification of HPV42 genome in DPA and non-DPA samples by capture-NGS. Controls consisted in nine cases of hidradenocarcinoma (cases 14-16, 18, 20-24), one atypical cystadenoma (case #13), one poroid

hidradenoma (case #19) and two adnexal carcinoma NOS (cases #12 and 18) Results are expressed as number of reads. Reads for *GAPDH*, *RAB7A* and *KLK3* served as control. Cases in which integration sites were identified are hatched. **B. Representation of the HPV42 integrated genomes.** Sequencing coverage and variants differing from the HPV42 reference are represented using IGV (Integrative Genome Browser). The HPV42 reference genome is depicted in a linearised form in the top. The early ("E", as in "E1") and late ("L", as in "L1") coding sequences (CDS) therein encoded are presented as boxes in the bottom. The sequencing coverage is displayed as a grey curve for three DPA cases and for one non-DPA case showing HPV42 integrations (DPA cases #2, #3 and #7 and non DPA case #12). For all of them, the height of the curve at a specific position is proportional to the fraction of number of Illumina reads covering it. The values in brackets (as "[0-4217]" for the non-DPA case) indicate the maximum and the minimum coverage values in positions along the genome. A flat background line (as between 1600bp and 3000bp in the non-DPA case), indicates absence of reads mapping that region, and are compatible with a loss of the corresponding viral genome stretch. The red arrows label junction positions between viral and human DNA identified with confidence in a significant fraction of reads, and are compatible with integration events at that given position. Coloured lines over the grey background indicate nucleotide polymorphisms in the HPV42 sequence actually recovered from the sample, compared to the reference sequence used for mapping. **C. HPV42 transcripts detection by *in situ* hybridization (RNA scope).** Untransfected and HPV42 E6-E7 transfected HeLa cells were used as negative and positive controls respectively.

Figure 4. Representative illustration of the morphologic and immunohistochemical features of the two primary cutaneous NUT carcinoma cases. Cases with *BRD3::NUTM1* and *NSD3::NUTM1* rearrangements are depicted. Microscopic examination of the cases

revealed strands and cords of poroid cells with ducts and keratocystic structures (white arrow). Immunohistochemical characterization revealed overexpression of NUT with preserved expression of YAP1 (C terminal part).

Figure 5. Representative illustration of the morphological and immunohistochemical features of the *NCOA4::RET* and *CCDC6::RET* rearranged cases. Microscopic examination revealed two cystic lesions, with gland formation, pseudopapillary projection, and anastomosing epithelial tufts. Apocrine differentiation and sign of decapitation secretion were observed. Immunohistochemical investigation revealed the presence of an external myoepithelial cell layer expressing p63**.**

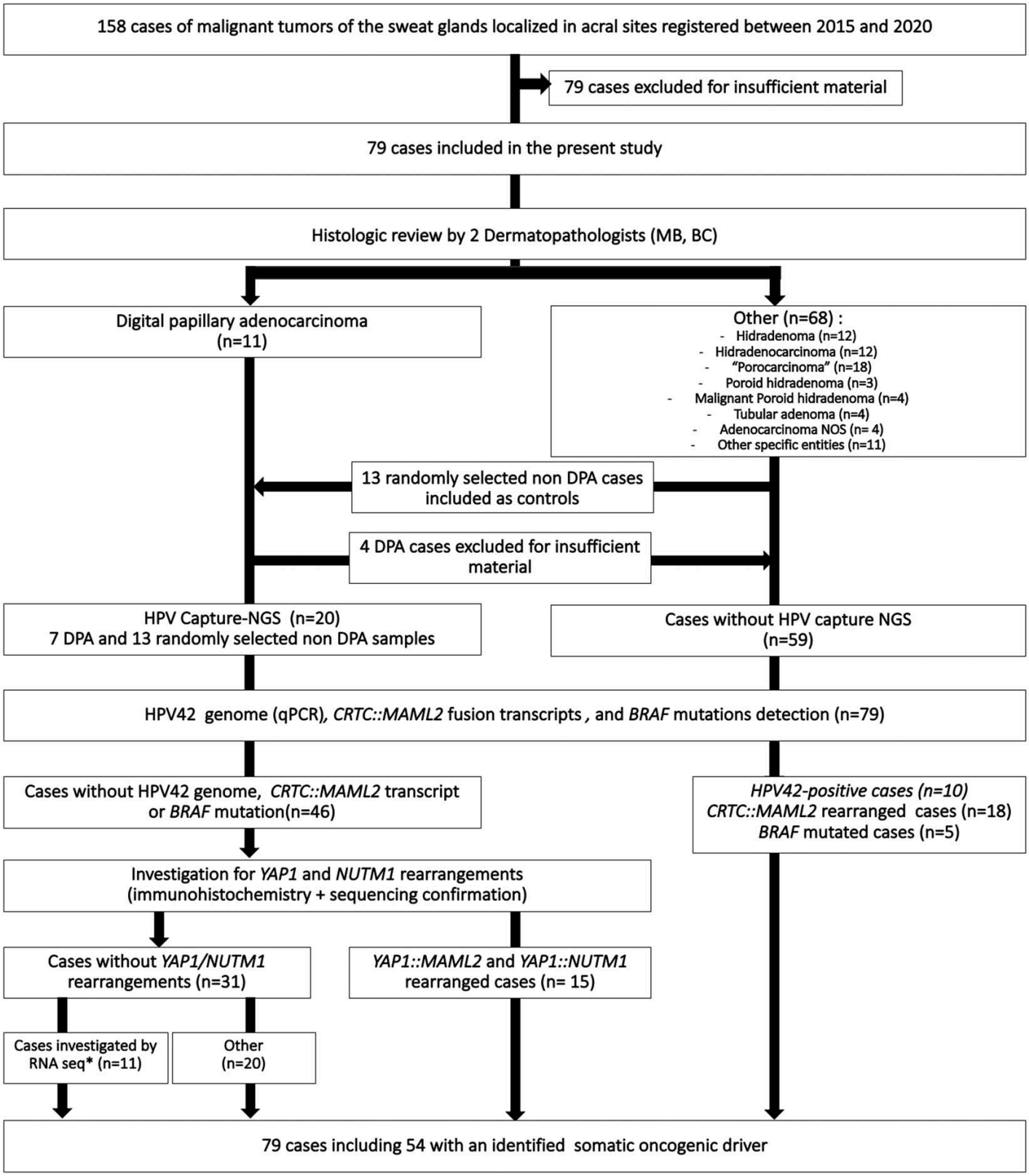

Figure 1
Kervarrec et al.
Am J Surg Pathol. 2023
doi: 10.1097/PAS.0000000000002098
Sweat Gland Tumors Arising on Acral Sites: A Molecular Survey

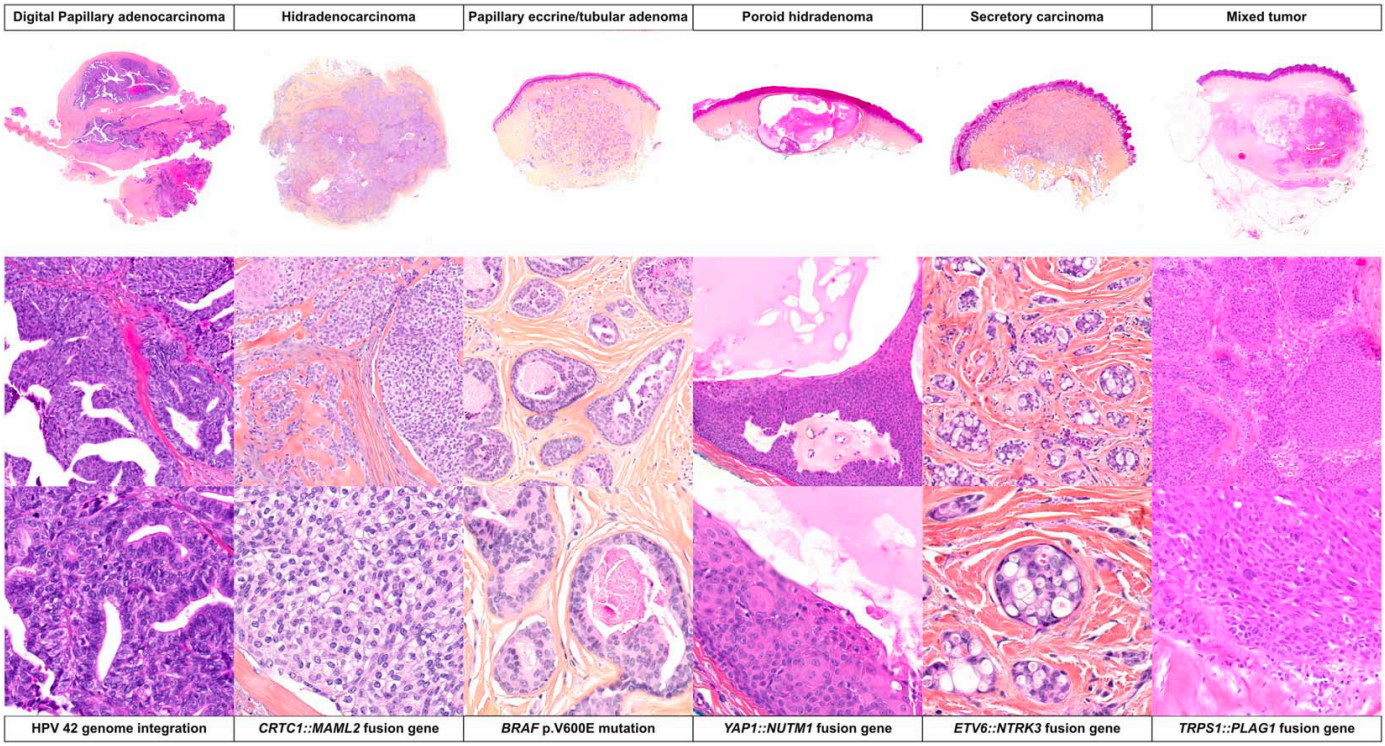

Figure 2
Kervarrec et al.
Am J Surg Pathol. 2023
doi: 10.1097/PAS.0000000000002098
Sweat Gland Tumors Arising on Acral Sites: A Molecular Survey

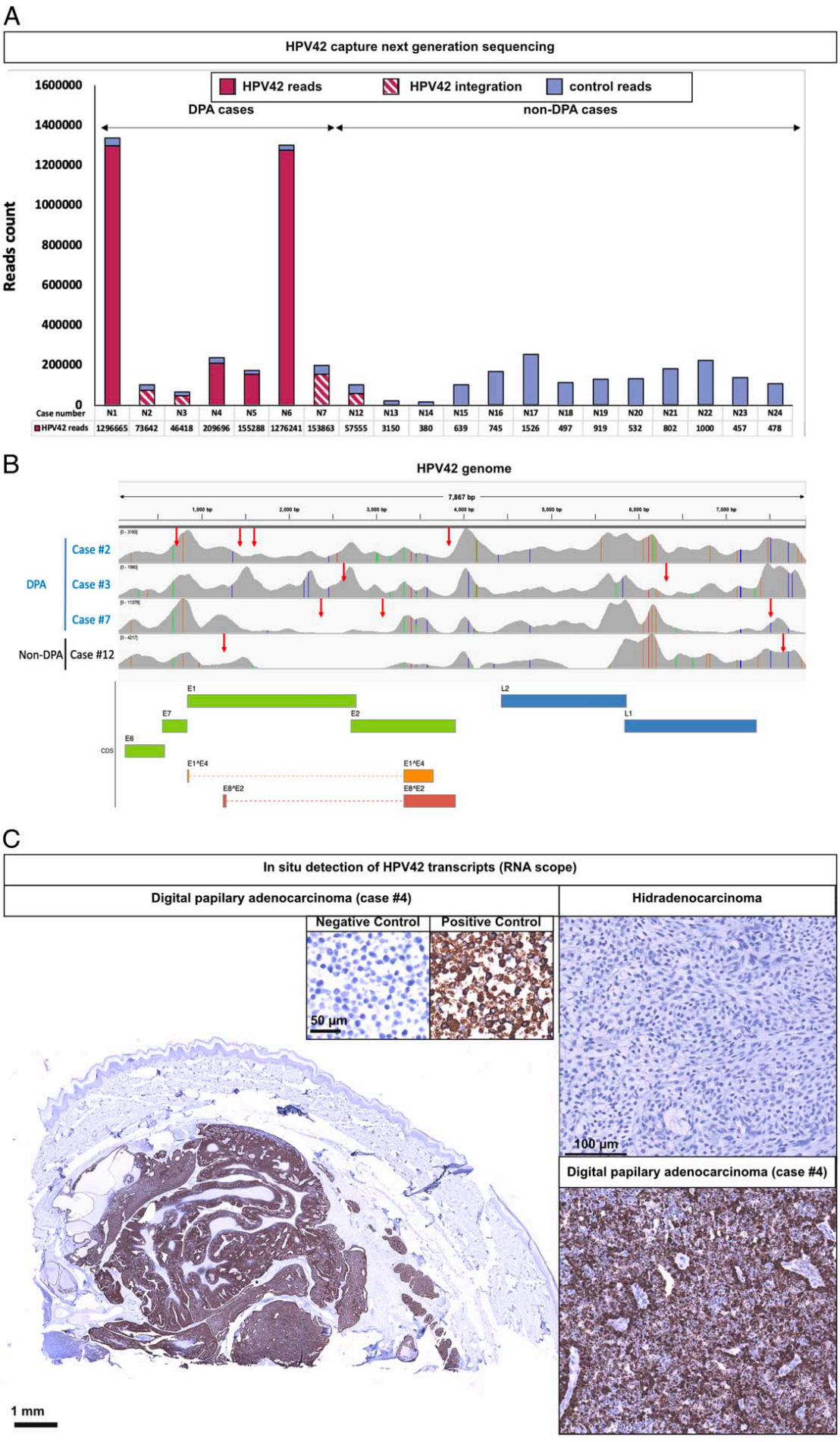

Figure 3
Kervarrec et al.
Am J Surg Pathol. 2023
doi: 10.1097/PAS.0000000000002098
Sweat Gland Tumors Arising on Acral Sites: A Molecular Survey

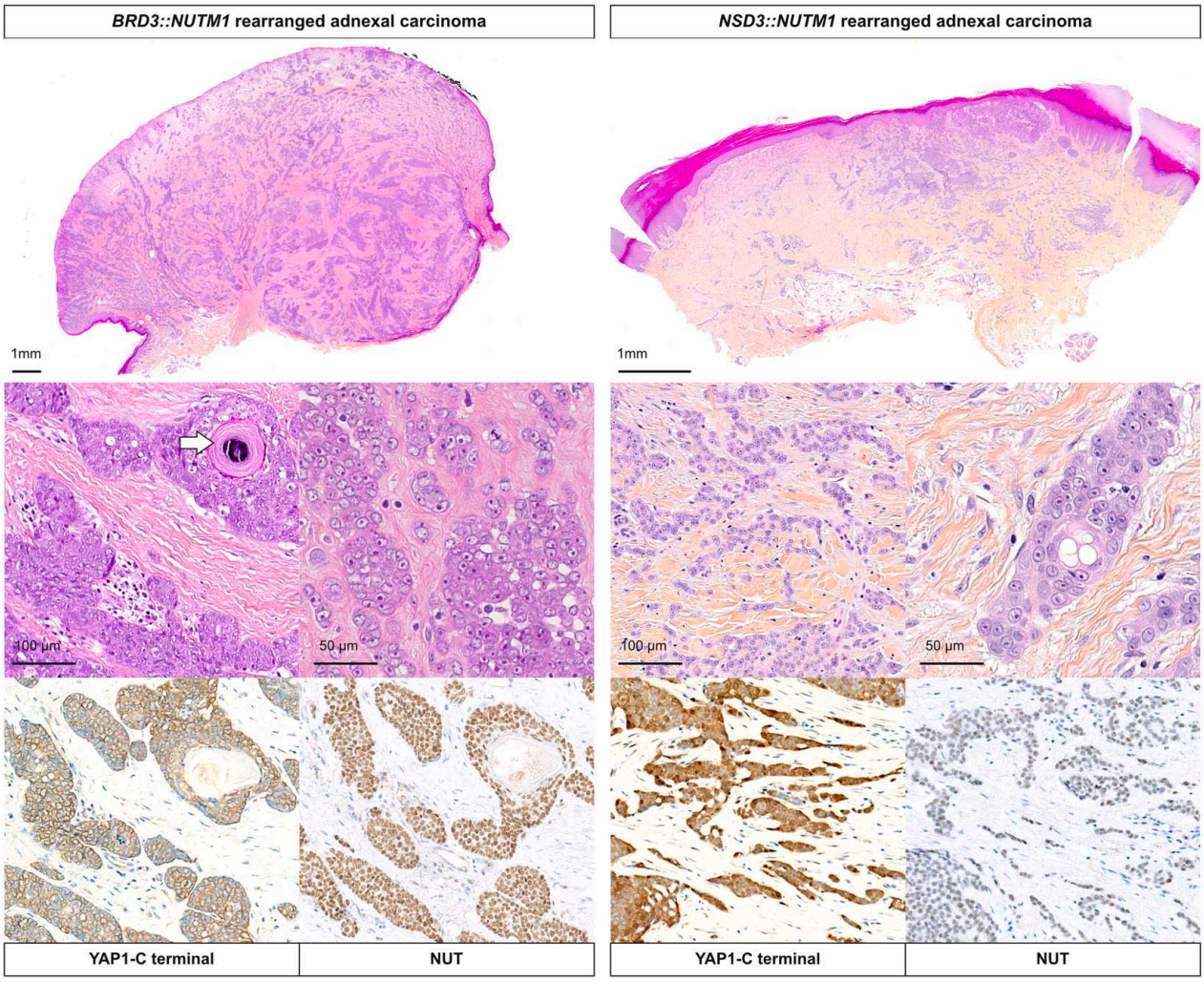

Figure 4
Kervarrec et al.
Am J Surg Pathol. 2023
doi: 10.1097/PAS.0000000000002098
Sweat Gland Tumors Arising on Acral Sites: A Molecular Survey

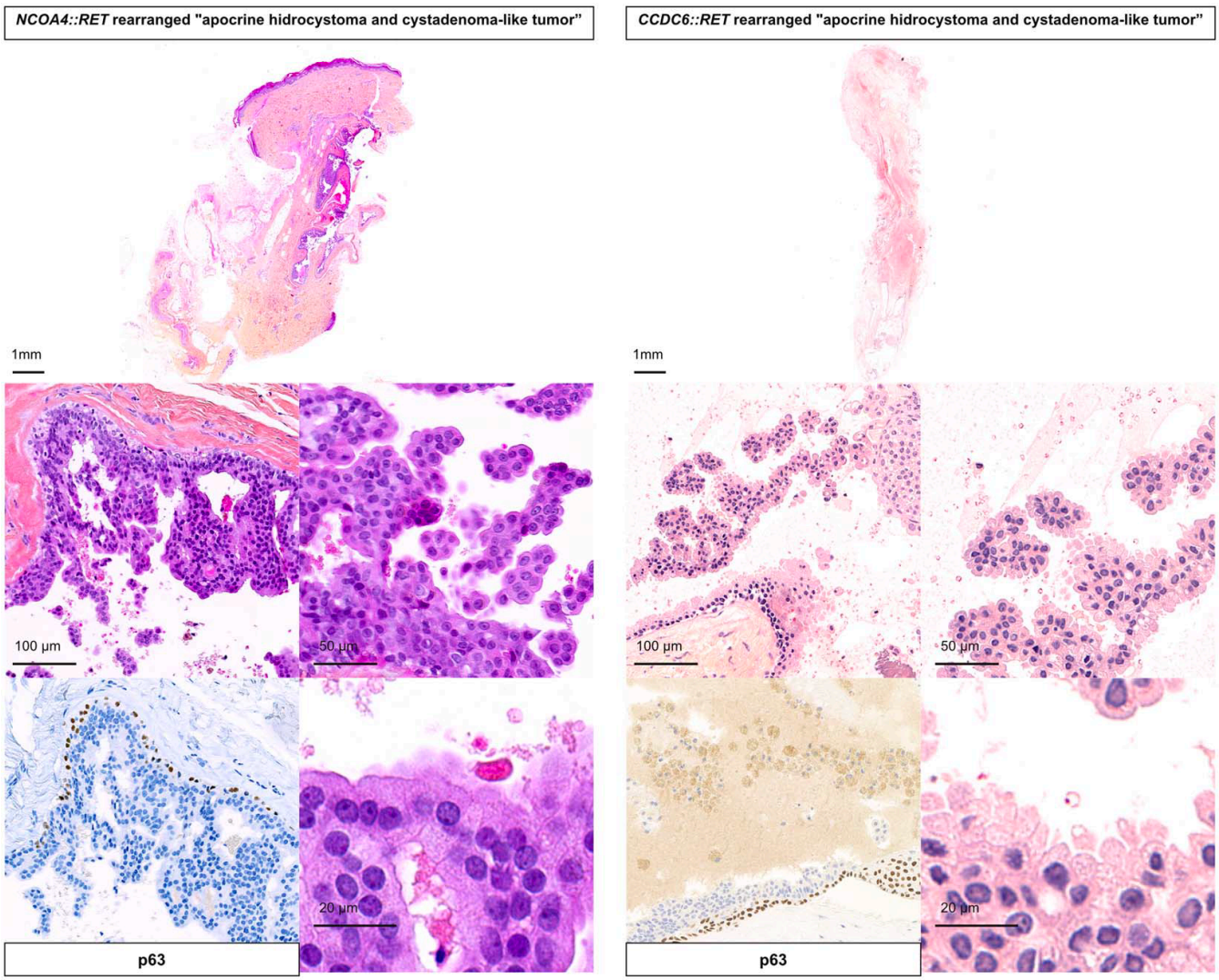

Figure 5
Kervarrec et al.
Am J Surg Pathol. 2023
doi: 10.1097/PAS.0000000000002098
Sweat Gland Tumors Arising on Acral Sites: A Molecular Survey

TABLE 1. Genetic Features of the Cohort According the Tumor Types

	n (%)											
Oncogenic driver	**HPV42 (quantitative PCR)**	***CRTC1::MAML2* (quantitative PCR)**	***B*RAF V600E (Pyroseq)**	***YAP1:: NUTM1* (RNA-seq)**	***YAP1:: MAML2* (RNA-seq)**	***BRD3:: NUTM1* (RNA-seq)**	***NSD3:: NUTM1* (RNA-seq)**	***TRPS1:: PLAG* (RNA-seq)**	***ETV6:: NTRK3* (RNA-seq)**	***NCOA4:: RET* (RNA-seq)**	***CCD6:: RET* (RNA-seq)**	**No identified alteration**
DPA (n = 11)	10 (91)	0	0	—	—	—	—	—	—	—	—	1 (9)
Hidradenoma (n = 12)	0	9 (75)	0	—	—	—	—	—	—	—	—	3 (25)
Hidradenocarcinoma (n = 12)	0	9 (75)	0	—	—	—	—	—	—	—	—	3 (25)
Porocarcinoma (n = 16)	0	0	0	3 (19)	5 (31)	—	—	—	—	—	—	8 (50)
NUT adnexal carcinoma (n = 2) (morphologically classified as porocarcinoma)	0	0	0	0	0	1 (50)	1 (50)				—	0
Tubular adenoma (n = 4)	0	0	4 (100)	—	—	—	—	—	—	—	—	0
Poroid hidradenoma (n = 3)	0	0	0	3 (100)	0	—	—	—	—	—	—	0
Malignant poroid hidradenoma (n = 4)	0	0	0	4 (100)	0	—	—	—	—	—	—	0
Secretory carcinoma (n = 1)	0	0	0	—	—	—	—	—	1 (100)	—	—	0
Cribriform carcinoma (n = 1)	0	0	0	—	—	—	—	—	—	—	—	1 (100)
Mixed tumor (n = 4)	0	0	0	—	—	—	—	3 (75)	—	—	—	1 (25)
Adenocarcinoma NOS (n = 4)	1 (25)	0	0	—	—	—	—	—	—	0	0	3 (75)
Hidrocystoma/cystadenoma* (n = 4)	0	0	0	—	—	—	—	—	—	1 (25)	1 (25)	2 (67)
Ambiguous (n = 1)	0	0	1 (100)	—	—	—	—	—	—	—	—	0
Total	11	18	5	10	5	1	1	3	1	1	1	22

*Including 2 atypical cases (#13 and #35).
— indicates nonevaluated.

Table 1
Kervarrec et al.
Am J Surg Pathol. 2023
doi: 10.1097/PAS.0000000000002098
Sweat Gland Tumors Arising on Acral Sites: A Molecular Survey

TABLE 2. Clinical, Microscopic, Immunohistochemical, and Molecular Features of DPA

	Case #1	Case #2	Case #3	Case #4	Case #5	Case #6	Case #7	Case #8	Case #9	Case #10	Case #11
Clinical features											
Age (y)	69	55	58	26	59	57	57	86	20	13	48
Sex	Male	Male	Male	Male	Male	Male	Male	Female	Male	Male	Male
Tumor characteristics*											
Site	Finger (3rd)	Finger (3rd)	Hand	Toe (1st)	Finger (1st)	Finger (2nd)	Finger(NA)	Hand	Toe (NA)	Toe (NA)	Finger (3rd)
Side	R	L	R	L	R	L	NA	R	L	NA	Right
Size (mm)	20	12	7	40	10	8	NA	13	NA	NA	4
Extension	T1N0M0	T1N0M0	T1N3M1	T4aNx	T1N0M0	T1N0M0	NA	T2N0M0	NA	NA	NA
Treatment	Surgery	Surgery	Surgery	Surgery	Surgery	Surgery	Surgery	Surgery	Surgery	Surgery	Surgery
Follow-up											
Duration (mo)	NA	13	34	120	36	22	5	NA	NA	NA	136
Local recurrence	NA	–	–	–	–	–	–	NA	NA	NA	–
Metastasis	NA	–	+ skin+lung	+ LN+bone+lung	–	–	–	NA	NA	NA	+ lung
Specific death	NA	–	+	–	–	–	–	NA	NA	NA	–
Microscopic features											
Architecture											
Solid	+	+	+	+	+	+	NA	–	NA	+	+
Cystic	+	+	+	+	+	+	NA	+	NA	+	+
Papillary structures	+	Few	+	+	+	+	NA	+	+	Few	+
Back to back glands	+	+	+	+	+	+	NA	–	+	+	+
Cytologic atypia	Moderate	Moderate	Moderate	Moderate	Moderate	Moderate	NA	Mild	Moderate	Moderate	Moderate
Other											
Apocrine differentiation	+	+	+	+	+	+	NA	+	+	+	+
Squamous metaplasia	–	–	–	–	–	–	NA	–	+	+	–
Necrosis	–	–	+	+	–	–	NA	–	–	+	–
Mitotic count (/10 HPF)	8	6	15	6	6	3	NA	1	1	1	5
Vascular invasion	–	+	+	+	–	–	NA	–	NA	–	–
IHC profile											
SOX10	Diffuse Myoepi. Cell.	Diffuse Myoepi. Cell.	Diffuse Myoepi. Cell.	Diffuse Myoepi. Cell.	Diffuse Myoepi. Cell.	Diffuse Myoepi. Cell.	Diffuse Myoepi. Cell.	Diffuse Myoepi. Cell.	Diffuse Myoepi. Cell.	Diffuse Myoepi. Cell.	Diffuse Myoepi. Cell.
p63											
Molecular features											
HPV42 (Capture-NGS)											
Virus status	EPI.	INT.	INT.	EPI.	EPI.	EPI.	INT.	NA	NA	NA	NA
Read Nb (HPV42)	1,296,665	73,642	46,418	209,696	155,288	1,276,241	15β,863				
HPV42 (quantitative PCR)											
Detection	pos	pos	pos	pos	pos	pos	pos	neg	pos	pos	pos
HPV42 (RNAscope)											
Detection	NA	pos	pos	pos	pos	pos	NA	NA	NA	NA	NA
Somatic alterations											
CRTC1::MAML2 re	–	–	–	–	–	–	–	–	–	–	–
*BRAF p.*V600E mu	–	–	–	–	–	–	–	–	–	–	–

*At the diagnosis time.

EPI indicates episomal; IHC, immunohistochemistery; INT, integrated; L, left; Mu, mutation; Myoepi. Cell., positivity restricted to the myoepithelial cell layer; NA, not available data; Nb, number; pos, positivity; R, right; Re, rearrangement; –, no alteration.

Table 2
Kervarrec et al.
Am J Surg Pathol. 2023
doi: 10.1097/PAS.0000000000002098
Sweat Gland Tumors Arising on Acral Sites: A Molecular Survey